

Structural Characterizations of Oligopyridyl Foldamers, α -Helix Mimetics

Jana Sopkova-de Oliveira Santos,^{*,†} Anne Sophie Voisin-Chiret,[†] Gregory Burzicki,[†] Laure Sebaoun,[†] Muriel Sebban,[‡] Jean-François Lohier,[§] Rémi Legay,[†] Hassan Oulyadi,[‡] Ronan Bureau,[†] and Sylvain Rault[†]

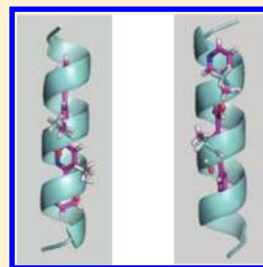
[†]Centre d'Etudes et de Recherche sur le Médicament de Normandie, UPRES EA-4258, FR CNRS INC3M, UFR des Sciences Pharmaceutiques, Université de Caen, bd Becquerel, 14032 Caen Cedex, France

[‡]Equipe Analyse et Modélisation Moléculaire, IRCOF UMR6014 CNRS-COBRA, Université de Rouen, rue Tesnière, 76821 Mont-Saint-Aignan, France

[§]Laboratoire de Chimie Moléculaire et Thio-organique, UMR CNRS 6507, FR CNRS 3038 INC3M, ENSICAEN - Université de Caen, 14050 Caen, France

S Supporting Information

ABSTRACT: Protein–protein interactions are central to many biological processes, from intracellular communication to cytoskeleton assembly, and therefore represent an important class of targets for new therapeutics. The most common secondary structure in natural proteins is an α -helix. Small molecules seem to be attractive candidates for stabilizing or disrupting protein–protein interactions based on α -helices. In our study, we assessed the ability of oligopyridyl scaffolds to mimic the α -helical twist. The theoretical as well as experimental studies (X-ray diffraction and NMR) on conformations of bipyridines in the function of substituent and pyridine nitrogen positions were carried out. Furthermore, the experimental techniques showed that the conformations observed in bipyridines are maintained within a longer oligopyridyl scaffold (quaterpyridines). The alignment of the synthesized quaterpyridine with two methyl substituents showed that it is an α -helix foldamer; their methyl groups overlap very well with side chain positions, i and $i + 3$, of an ideal α -helix.



■ INTRODUCTION

A majority of processes in living cells are controlled by proteins, sometimes alone, but more often in concert with other partners. The formation of protein–protein complexes is essential for numerous regulatory processes in cells and paramount for survival. Thus, modulation of protein–protein interactions (PPIs) is a valuable tool in understanding biochemical pathways and may lead to the development of new therapeutic candidates.

Indeed, there are numerous examples in the literature of using antibodies¹ or medium-size peptides to inhibit particular protein–protein assemblies. Although antibodies offer the advantage of having very high affinities for their target proteins, they are expensive to produce, have low oral bioavailability, and have undesired side effects.² Medium-size peptides exhibit several disadvantages compared to small molecules. They are generally inactive by the oral route, which is the most commonly accepted entry, because they show unfavorable pharmacokinetic properties: low capacity to cross membranes, particularly from the digestive tract to the bloodstream, and low systemic stability.³ Medium-size peptides cannot lead to delayed or long-acting effects.⁴

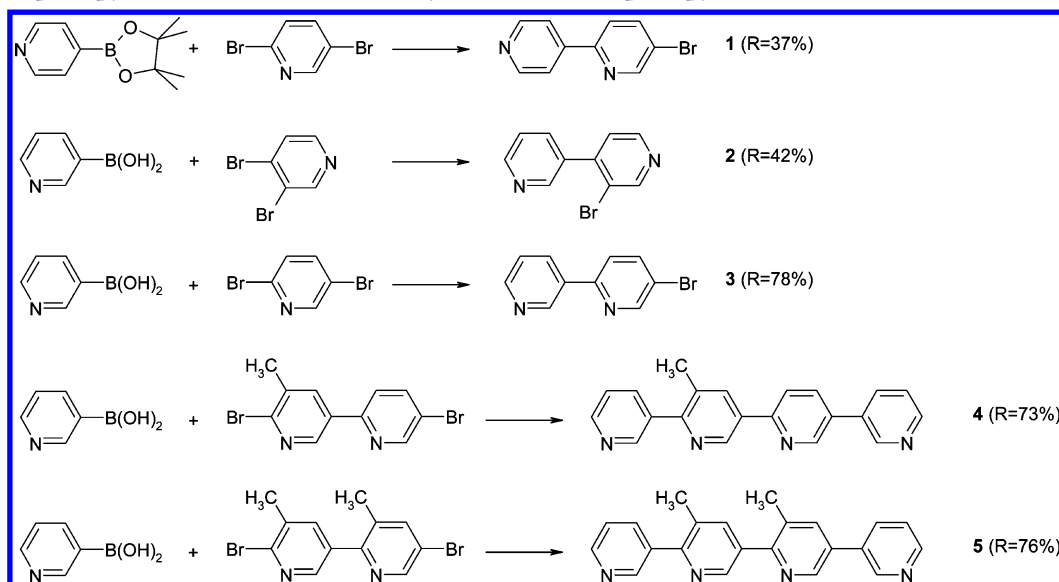
An alternative approach involves the design and the synthesis of small molecules able to disrupt PPIs. However, to date, this remains an issue.⁵ The structures of many oligomeric proteins and protein–protein complexes show them to have generally large and flat interfaces, making the rational design of small molecules able to mimic these surfaces a difficult prospect.

Small molecular scaffolds are often limited in their affinity and selectivity toward these shallow topological features and large surface areas. However, synthetic scaffolds that mimic only the key elements of a protein surface (named “Hot Spots”) can potentially lead to small molecules having almost the full activity of a protein domain, only a fraction of the molecular weight, and no peptide bonds.⁶ To date, the majority of small molecule drug design successes correspond to bimolecular complexes built by analyzing the interactions of regular protein secondary structure elements, such as surface-exposed extended β -strand segments and β -turns. In these cases, the designed nonpeptide molecules retained the orientation of the amino acid side chains in a strand or a turn.⁷ However, α -helices are the most common protein secondary structures, accounting for over 40% of polypeptide amino acids in natural proteins.⁸ One strategy for the design of agents able to disrupt α -helix interactions therefore involves the mimicry of side-chain residues on one face of an α -helix. Surprisingly, there are only few examples of small molecules mimicking a protein α -helix, and a majority of them are based on an approach in which hydrogen bonding propensities that control its folding into a desired conformation are built into the molecule. Among the previously reported α -helix mimetic scaffolds, we can mention,

Received: September 9, 2011

Published: December 24, 2011

Scheme 1. Synthesis of 5-Bromo-2,4'-bipyridine (1),^a 3'-Bromo-3,4'-bipyridine (2),^a 5-Bromo-2,3'-bipyridine (3),^a 3'-Methyl-3,2':5'2'':5'3'''-quaterpyridine (4),^b and 3',3''-Dimethyl-3,2':5'2'':5'3'''-quaterpyridine (5)^b



^aReaction conditions and reagents: pyridylboronic acid or ester 1.2 equiv dihalopyridine or dihalobipyridine 1.0 equiv, Na₂CO₃aq. 2.5 equiv, Pd(PPh₃)₄ 0.05 equiv, 1,4-dioxane, reflux. ^bReaction conditions and reagents: 3-pyridylboronic acid 2.5 equiv, dihalobipyridine 1.0 equiv, Na₂CO₃aq. 5.0 equiv, Pd(PPh₃)₄ 0.1 equiv, 1,4-dioxane, reflux.

for example, indane,⁹ biphenyl,⁷ benzamides,¹⁰ polycyclic ether,¹¹ and the ABT-737 family,¹² promising inhibitors disrupting α -helix/ α -helix interactions occurring in apoptosis.

Hamilton and co-workers have designed a preorganized α -helix mimetic terphenyl^{13,14} by synthesizing the first entirely nonpeptidic scaffold from 3,2',2''-trisubstituted terphenyl derivatives. This scaffold mimics substituents *i*, *i* + 3, and *i* + 7—one ridge—of an α -helical dodecapeptide.¹⁵

Our efforts in the design of novel α -helix mimetics that disrupt PPIs were prompted by the terphenyl α -helix mimetic concept. Hamilton and co-workers observed that the terphenyl scaffolds are not rigid. For example, they could adopt both right- and left-handed twists, and the possibility of mutual phenyl orientations is limited. Various other organic scaffolds have therefore been proposed, including a terpyridyl scaffold.¹⁶

In our study, we assessed the ability of oligopyridyl scaffolds to mimic the α -helical twist. The first main objective was to define all possible conformations associated with oligopyridines. We first carried out detailed studies using quantum mechanics calculations of bipyridine conformations as a function of nitrogen and substituent positions. We then compared the theoretical results with experimental 3D data obtained on the synthesized bi- and quaterpyridines using two methods, X-ray diffraction (solid state) and NMR (liquid state). These experimental structural data were then correlated with an α -helix side chain distribution.

MATERIALS AND METHODS

Conformational Analysis. 3D models for every possible bipyridines as a function of the pyridyl nitrogen and substituent positions were built using the Discovery Studio software.¹⁷ This corresponds to 30 bipyridine models substituted with a bromine or methyl group. The Cartesian coordinates of each model were used as input for the *ab initio* simulation.

All *ab initio* calculations reported in the present study were carried out using the Gaussian 98 software.¹⁸ Potential energy

scan (PES) studies of all bipyridines substituted with a bromine or methyl group consisted of a (−180°, +180°) geometry optimization with the specified coordinate freezing and a 5° increment in order to obtain the internal energy barrier to rotation at the HF/6-31G level.

General Procedure for Suzuki–Miyaura Cross-Coupling Reactions. Commercial reagents were used as received without further purification. A mixture of pyridylboronic acid or ester (1.2 equiv), dihalopyridine (1.0 equiv), tetrakis(triphenylphosphine) palladium (5 mol %), and aqueous Na₂CO₃ (2.5 equiv) in 1,4-dioxane was heated to 80 °C for 1 h, then under reflux until the complete consumption of dihalopyridine (TLC). Crude products were purified on silica gel column chromatography to give 5-bromo-2,4'-bipyridine¹⁹ (1), 3'-bromo-3,4'-bipyridine (2), and 5-bromo-2,3'-bipyridine^{20,21,19} (3) with, respectively, 37%, 42%, and 78% yields (see Scheme 1).

The same procedure was used with 3-pyridylboronic acid (2.5 equiv), dihalobipyridine²² (1.0 equiv), tetrakis(triphenylphosphine) palladium(0) (10 mol %), and aqueous Na₂CO₃ (5.0 equiv) in 1,4-dioxane at reflux (see Scheme 1) to produce 3'-methyl-3,2':5'2'':5'3'''-quaterpyridine (4) and 3',3''-dimethyl-3,2':5'2'':5'3'''-quaterpyridine (5) with, respectively, 73% and 76% yield.

Melting points were determined on a Kofler heating bench. IR spectra were recorded on a Perkin-Elmer BX FT-IR spectrophotometer. ¹H NMR (400 MHz) and ¹³C NMR (100 MHz) spectra were recorded on a JEOL Lambda 400 spectrometer. Mass spectra were recorded on a JEOL JMS GCMate spectrometer at 70 eV ionizing potential (EI) and with pfk as an internal standard for the high-resolution procedure or were performed using a LC-MS Waters alliance 2695 (ESI+) spectrometer. Chromatography was carried out on a column using flash silica gel 60 Merck (0.063–0.200 mm) as the stationary phase. Thin layer chromatography (TLC) was performed on 0.2 mm precoated plates of silica gel 60F-264 (Merck), and spots were visualized using an ultraviolet-light lamp.

X-Ray Diffraction. Single crystal X-ray analysis was carried out using graphite-monochromatized Mo $K\alpha$ radiation on a Bruker-Nonius Kappa II diffractometer equipped with a CCD area detector. The crystal structure was solved by direct methods using the SHELX97 package (SHELXS²³) and refined using SHELXL.²⁴ The refinement was based on F_2 for all reflections, and all non-hydrogen atoms were refined anisotropically. Hydrogen atom positions were determined either *via* difference Fourier maps and refined with isotropic atomic displacement parameters or were calculated and fixed in the ideal geometry, depending on data quality.

NMR Measurements. All NMR experiments were carried out using a Bruker AVIII 600 spectrometer (Bruker, Wissembourg, France) equipped with a 10 A gradient amplifier and a 5 mm CPTXI{¹H, ¹³C, ¹⁵N} including shielded z-gradients. Solutions with concentrations in the range 50–80 mg·mL⁻¹ in CDCl₃ were used. Experiments were carried out at 600 MHz for ¹H and 150 MHz for ¹³C. ¹H and ¹³C chemical shifts were referenced according to the CDCl₃ solvent signal used as a secondary internal reference (¹H, δ = 7.26 ppm; ¹³C, δ = 77 ppm, with respect to TMS, 0 ppm).

The 1D and 2D NMR spectra were obtained at 298 K. Complete assignment of all protons and carbons was carried out using conventional 2D experiments: COSY (¹H–¹H), TOCSY (¹H–¹H), NOESY (¹H–¹H), HSQC (¹H–¹³C), and HMBC (¹H–¹³C). For all 2D spectra, a total of 2048 points in F2 and 512 experiments in F1 were recorded. For the HMBC experiment, an evolution delay of 65 ms was chosen in such a way that correlations involving long-range J coupling around 8 Hz could be observed. The NOESY and the TOCSY experiments were performed using mixing times of 1.5 s and 200 ms, respectively. Processing and analysis of the NMR spectra was performed with the Topspin 2.1 software from Bruker on a PC workstation.

Molecular Modeling with NMR Constraints. Three dimensional NMR structures of quaterpyridines were refined using the CHARMM program with potential function parameter set 22 from Discovery Studio. The Discovery Studio program was also used to derive CHARMM force field parameters for the quaterpyridines applying MMFF partial charges. The ring twist angles in the two studied quaterpyridines are the torsions with the lowest energy barriers according to our theoretical calculations (five of them with $\Delta E \sim 3$ kcal/mol and one with $\Delta E \sim 4.5$ kcal/mol). For this reason, we used only the force field derived by the Discovery Studio without the introduction of supplementary dihedral force field parameters based on our mechanic quantum simulations. To verify the molecular-mechanics force fields obtained, the structures were energy minimized, and their molecular geometry was compared with the X-ray structures. The root-mean-square deviation (RMSD) between the X-ray and the optimized NMR structure was <0.1 Å for both structures.

During all CHARMM simulations, NOE (distance) restraints were applied with a force constant of 25 kcal/mol. Starting from the energy minimized X-ray structure, a dynamics simulation of 50 ns was carried out for each quaterpyridine at 300 K, with a time step of 1 fs. The dynamics were preceded by a heating (during 6 ps) and an equilibration (50 ps) step.

During the production phase, configurations were saved every 5 ps and energy minimized to a root-mean-square gradient of less than 0.001 kcal/(mol·Å²). The 10 lowest-energy configurations obtained for each quaterpyridine were used in the subsequent analysis. The selected structures were analyzed and displayed using Discovery Studio.

RESULTS AND DISCUSSION

Since the critical interactions for α -helix recognition often involve the side chains of residues on one helical face (i , $i + 3$ and/or $i + 4$ and $i + 7$), it is possible to design an appropriate scaffold with limited conformations that can orient the attached functional groups to correctly resemble an α -helical surface (Figure 1). In the case of the oligophenyl scaffold, the adjacent

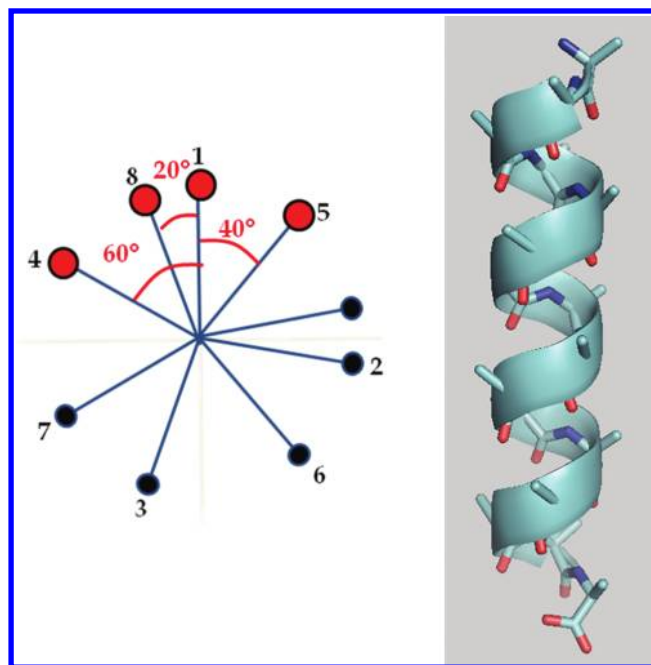


Figure 1. The geometry of side chains on one face of an α -helix.

phenyl rings are balanced by two competing factors: (i) a symmetric interaction between the π orbitals of the aromatic rings and (ii) a steric repulsion between overlapping *ortho* hydrogen atoms and substituents.¹⁶ In the case of oligopyridines, in addition to these two effects, the twist between the adjacent rings will also be influenced by the position of the nitrogen atoms in the rings. We therefore carried out this study to evaluate the advantages and disadvantages of the oligopyridyl compared to the oligophenyl scaffold.

What Is the Influence of Nitrogen and Substituent Positions on the Twist Angle between Adjacent Pyridine Rings? This analysis was started by theoretical simulations carried out on a simple system constituted of two pyridine rings and substituted by a bromine atom. In total, 30 models were built, 12 with bromine in the *ortho* and *meta* positions and 6 in the *para* position (see Table 1). For each model, the internal barrier of potential energy was calculated by *ab initio* simulation as a function of the torsion angle between the two rings. The results are summarized in Table 1 and Figure 2, showing that the 30 models can be divided into six groups depending on the preferential twist angle between adjacent pyridine rings and the height of the energy barrier associated with the bipyridine twist. Thus, the bipyridine system substituted by bromine can adopt six different conformations compared with only two possible in the biphenyl system (Figure 2). The bromine substituent represents a relatively important steric hindrance related to its bond length ($d_{\text{Car-Br}} \sim 1.91$ Å) and the van der Waals radius (195 pm) due to its three lone pairs. The nitrogen has a lone pair, and it introduces a negative partial charge in the ring. So in

Table 1. Structural Parameters of Minimum Energy Conformers of Br Substituted Bipyridine Obtained from PES at the HF/2-31G Level^a

Compound and preferred orientation of rings with respect to N		Preferential angle between the ring planes	Potential Energy Barrier [kcal/mol]
	Preferred orientation		
		$\pm 50^\circ$ ($\pm 35^\circ - \pm 70^\circ$)	3
		$\pm 50^\circ$ ($\pm 35^\circ - \pm 60^\circ$)	from 6.0 to 8.0
		Large minimum from ± 60 to ± 90 ($\pm 55^\circ - 90^\circ$)	10.5
		Co-planar ($0^\circ - \pm 30^\circ$)	4.5-5.5
		Co-planar ($0^\circ - \pm 10^\circ$)	12
		Co-planar ($0^\circ - \pm 40^\circ$)	9.5

^aValues in parentheses correspond to a 0.5 kcal/mol limit.

our bipyridine system, a competition of three phenomena occurs: (i) symmetric interaction between π orbitals of rings, (ii) steric repulsion between overlapping *ortho* hydrogens and the *ortho* substituent, and (iii) electrostatic repulsion.

When the four atoms in the direct neighborhood of the junction are the carbons, the rings twist angle is about 50° ($\Delta E \sim 3$ kcal/mol, Table 1). In this case, the steric repulsion dominates somewhat on the π -orbitals' symmetric interaction. The introduction of a bromine atom at the *ortho* position causes a more important steric repulsion ($\Delta E \sim 10.5$ kcal/mol, Table 1) and introduces therefore a greater twist angle of about 60° – 90° .

When the nitrogen atoms of both rings lie in the direct neighborhood of the bipyridine junction, independent of the position of the bromine substituent, the pyridine rings are always strongly constrained in the coplanar position ($\Delta E \sim 10$ – 12 kcal/mol), and the nitrogen lone pair repulsion as well as weak electrostatic interactions between N and CH cause the nitrogen atoms to be situated on the opposite site of the junction.

In the case that only one nitrogen of the two rings is in the *ortho* position of the junction and the bromine substituent is in the *meta* or *para* position, the two rings are also coplanar ($\Delta E \sim 4.5$ – 5.5 kcal/mol). With the bromine substituent in the *ortho* position, the situation is more complex: (i) When the

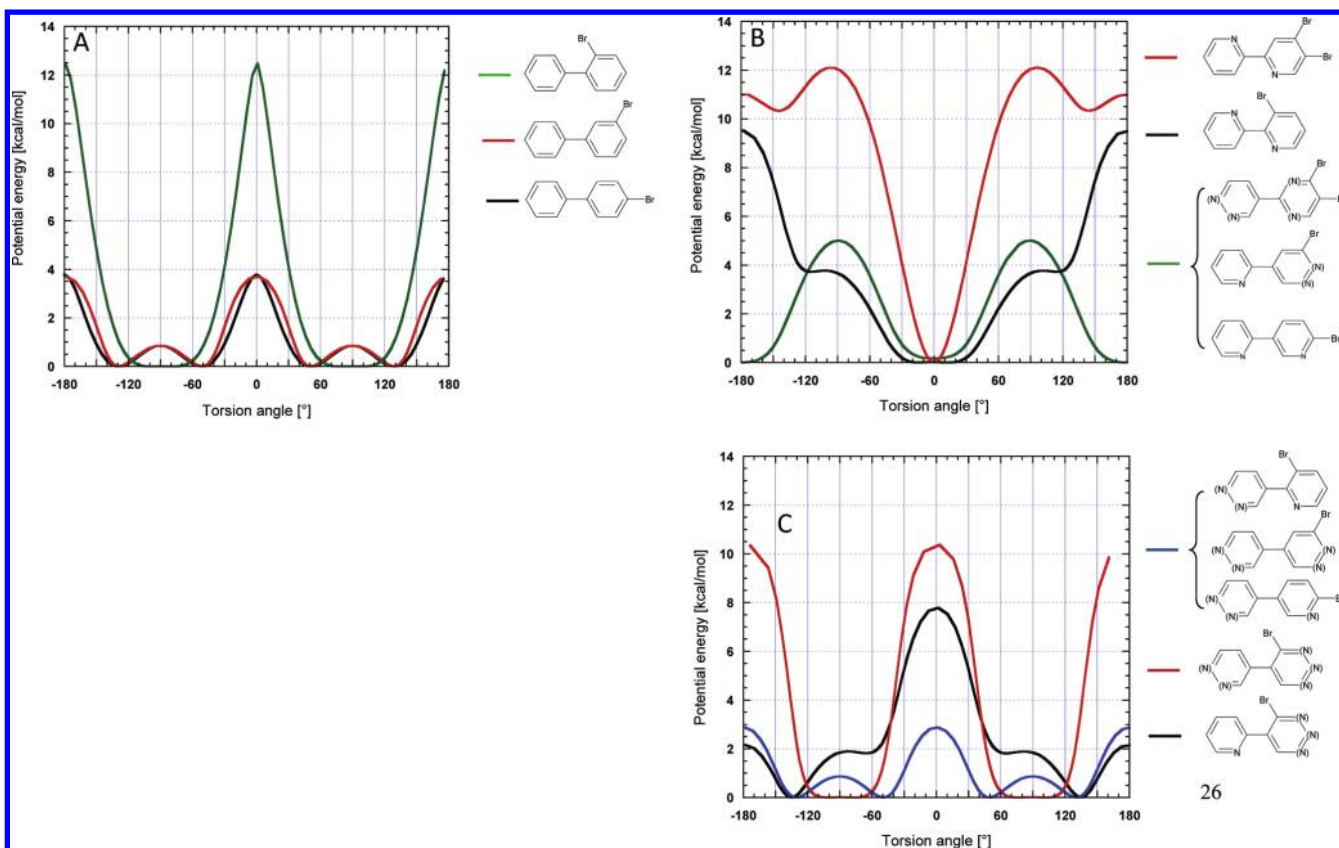


Figure 2. Evolution of potential energy as a function of torsion angle between the ring: (A) biphenyl system substituted by bromine atom and (B, C) bipyridine system with bromine substituent.

nitrogen of the pyridine without a bromine substituent is in the *ortho* position, the twist angle is about 50° due to steric and lone pair (electrostatic) repulsion between bromine and nitrogen ($\Delta E \sim 6\text{--}8$ kcal/mol), and the pyridine nitrogen in this case is always on the opposite site of junction with respect to the bromine. (ii) When the nitrogen of the pyridine with the substituent is in the *ortho* position of the junction, there is steric repulsion of the substituent and the ring's twist angle is about 50° , but in this case the lone pair repulsion does not occur and $\Delta E \sim 3$ kcal/mol (Table 1, Figure 2).

To mimic a side chain distribution of an α -helix, a twist angle between two rings close to 40° ($i + 3$) or 60° ($i + 4$) is appropriate (see Figure 1). The simulations showed that we are able to introduce a twist angle of about 50° , with an energy barrier that is more or less high ($\Delta E \sim 3\text{--}8$ kcal/mol) and a twist angle of about 60° with a higher energy barrier ($\Delta E \sim 10.5$ kcal/mol). However, the theoretical simulations showed that all bipyridines can rotate left and right with equal probability, as in the biphenyles.

All bromobipyridines were synthesized in our laboratory with good yields. One disadvantage of the terphenyl scaffolds described by Hamilton is the rather lengthy, multistep synthetic approach needed for its assembly.^{15,25} Therefore, our oligopyridines are simply assembled by a cross-coupling reaction. Our laboratory specializes in the preparation of pyridyl boronic species^{26–29} and in the study of their ability to be good cross-coupling partners.^{30–32} An iterative, regioselective, and highly flexible synthesis of new halo-oligopyridines using the Suzuki–Miyaura cross-coupling reaction in a strategy called the Garlanding concept was recently reported by our laboratory.³³

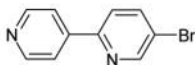
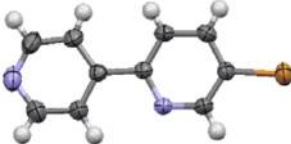
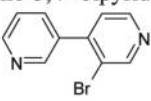
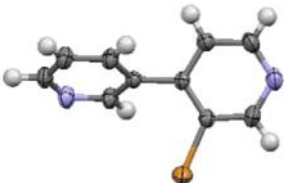
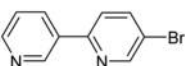
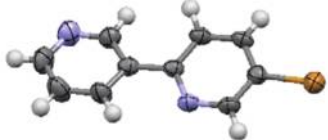
The regioselective control of the pyridine–pyridine linkage is complex to handle, but our cross-coupling strategy is efficient,

leading to a regioselective coupling. On the one hand, this strategy takes into account the nature and the position of the halogen on the pyridine ring (especially if there are several halogen atoms) and, on the other hand, the nature and the position of the boronic species on the pyridine ring.

Besides that, several trials of cross-coupling procedures using different reaction conditions (base, catalyst, solvent, temperature, and reaction time) were attempted. Accordingly, we have determined the optimal conditions, where Na_2CO_3 was used as a base, $\text{Pd}(\text{Ph}_3)_4$ as a catalyst, and 1,4-dioxane as a solvent. The completion of the reaction was determined by the total consumption of the halide (checked by thin layer chromatography). The synthesis of bipyridines 1 and 3 is known in the literature^{19–21} but the bipyridine 2 is a new compound.

Of all bromobipyridines synthesized, suitable crystals were obtained for three derivatives (Table 2). The crystal visualization under the microscope showed for each derivative only one kind of crystal (needles), and they are probably no polymorphism. We were thus able to compare our theoretical results with experimental values obtained from the crystal structures (Table 2). For each compound, the crystal space group contained a symmetric center, and consequently two axial enantiomers are present in each crystal: one has a right-handed twist (Ring1–Ring2–P), while the second is left-handed (Ring1–Ring2–M). According to the theoretical result, the rings of 5-bromo-2,4'-bipyridine (1) should adopt a coplanar position, and they are indeed coplanar in the crystal structure (twist angle between the ring planes is $\pm 1.27^\circ$), while the rings of 3'-bromo-3,4'-bipyridine (2) should adopt an orientation between $\pm 55^\circ$ and $\pm 90^\circ$, and the twist plane angle is about $\pm 55^\circ$. For 5-bromo-2,4'-bipyridine (3), two conformations were observed in the asymmetric unit of 3, and both have a twist

Table 2. ORTEP View of the Crystal Structures with the Predicted and Experimental Twist Angle Values

	ORTEP diagramme	Theoretical twist angle	Twist angle from X-ray structure
5-bromo-2,3'-bipyridine (1) 		Co-planar (0°- ±30°)	±1.27°
3'-bromo-3,4'-bipyridine (2) 		Between ± 55° and ±90°	±54.52°
5-bromo-2,4'-bipyridine (3) 		Co-planar (0°- ±30°)	±14.99° ±13.09°

angle of about 15° (±15° and ±13°, respectively), which is in agreement with the theoretical value of 0°–30°. Therefore, we can conclude that the theoretical and experimental values are consistent for three compounds.

Will the Energy Barrier Change if the Bromine, an Electronegative Substituent, Is Replaced by a Methyl One? As the aim of our study is to synthesize oligopyridines substituted by various side chains, the next step was an evaluation of what changes when the substituent is a hydrophobic methyl group. The theoretical calculation showed that there are no differences for *para* and *meta* substituent positions, but some differences were observed for the *ortho* position (Table 3), due to the absence of a lone pair on the methyl substituent.

The simulation results showed first that, contrary to bromo bipyridines, all methyl bipyridines in which one nitrogen is situated in the direct neighborhood of the bipyridine junction yield the same result, a preferential twist angle of 50° with an energy barrier of about 3 kcal/mol, which is due to the absence of a lone pair (electrostatic) repulsion between methyl and pyridine nitrogen. The absence of a lone pair on the methyl group influences also the profile of the energy barrier of the methyl bipyridines in which the nitrogen lies further from the bipyridine junction, the energy minimum is more narrow (from 50° to 90°), and its height is lower ($\Delta E \sim 9.5$ kcal/mol, Table 3). In conclusion, the bipyridine system substituted by a methyl group has generated five different ring orientations, and therefore it allows us to play more subtly with the distribution of substituents on the oligopyridyl compared to oligophenyl scaffolds (the biphenyl system generate only two different orientations—Figure 2). However, the highest energy barrier in biphenyl as in bipyridine is the same level.

Will the Energy Barrier Observed for a Bipyridine Be the Same if It Is Included in an Oligopyridyl Scaffold?

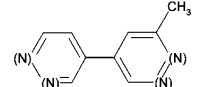
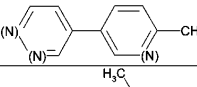
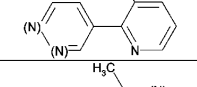
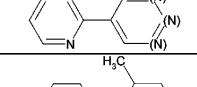
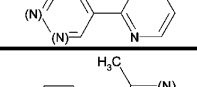
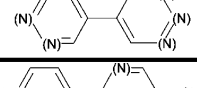
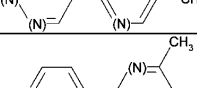
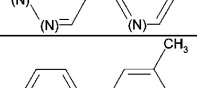
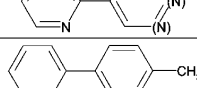
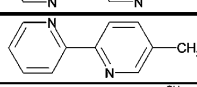
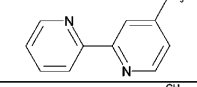
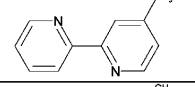
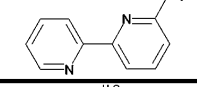
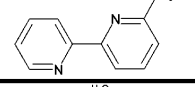
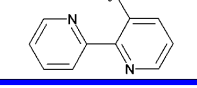
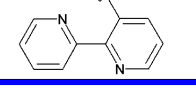
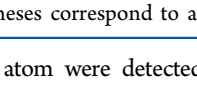
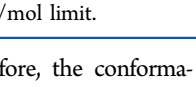
The implementation of the Garlanding concept^{22,33,34} was used to prepare two new terpyridines with good reactivity to introduce the two pyridin-3-yl moiety.²² 3'-Methyl-3,2':5',2'':5'',3'''-quaterpyridine (4) and 3',3''-dimethyl-3,2':5',2'':5'',3'''-quaterpyridine (5) were synthesized and successfully crystallized (Figure 3). As in the case of bipyridine, only one kind of crystal was observed under the microscope for both quaterpyridines.

The crystal structure of 4 and 5 shows that the pyridines in the scaffold turn as expected, and once more as in the case of bipyridine, the space groups of both crystals are center-symmetric, and so two axial enantiomers are presents in the crystals. Therefore, we compared first the theoretical prediction of twist angles from the bipyridyl model with the twist angles observed in the crystal structures 4 and 5 at the absolute value level. Together, we saw only one small difference in 4 with respect to the theoretical value. The middle twist angle should be of about 0°–35° according to the simulation, but in the crystal structure, we observed an angle of about 38°.

To verify if the bipyridyl model is adequate to use for the prediction in the quaterpyridine, the energy barrier for each junction in the complete, four-unit model of 4 and 5 was calculated anew. The simulation results showed only minor differences in the height of energy barriers and no differences in the position of energy minima with respect to the predictions from bipyridyl model. Thus, we can conclude that the bipyridyl model is applicable for longer pyridyl chains.

Another fact that needs to be considered is that the final structure in the crystal is also influenced by intermolecular interactions. Indeed, in the crystal packing of 4 and 5, weak electrostatic interaction between the pyridine nitrogen and

Table 3. Structural Parameters of Minimum Energy Conformers of Methyl Substituted Bipyridine Obtained from PES at the HF/2-31G Level^a

Compound and preferred orientation of rings with respect to N		Preferential angle between the ring planes	Potential Energy Barrier [kcal/mol]
	Preferred orientation		
		$\pm 50^\circ$ ($\pm 35^\circ - \pm 70^\circ$)	3
			
			
			
			
		Large minimum from ± 70 to ± 90 ($\pm 55^\circ - \pm 90^\circ$)	9.5
		Co-planar ($0^\circ - \pm 35^\circ$)	From 4.5 to 5.5
			
			
			
		Co-planar ($0^\circ - \pm 5^\circ$)	12
			
			
		Co-planar ($0^\circ - \pm 10^\circ$)	14

^aValues in parentheses correspond to a 0.5 kcal/mol limit.

aromatic carbon atom were detected. Therefore, the conformations of our oligopyridines found by the X-ray analysis were compared with their conformations in solution. In order to characterize the three-dimensional structure of **4** and **5** in solution, we carried out a structural NMR study. In the first step, assignment of the ¹H NMR spectra of **4** and **5** was done by ¹H–¹H correlation spectroscopy (COSY and TOCSY) and (¹H–¹³C) heteronuclear HSQC and HMBC, as well as (¹H–¹H) nuclear Overhauser effect spectroscopy (NOESY). The proton chemical shift values and coupling constants of **4** and **5** are summarized in Table 4.

The most important information regarding the structures of **4** and **5** was given by the two-dimensional (¹H–¹H) NOESY

spectrum. Quantitative analysis of the interproton distances was carried out by volume quantification of the correlation peaks observed in the NOESY spectrum. For the conversion of the NOE measurement to distance restraints, the usual relationship between the NOE intensity and the distance between a pair of nuclei for an isolated pair of spins was used:

$$r_{ij} = r_{kl} \left(\frac{\text{NOE}_{kl}}{\text{NOE}_{ij}} \right)^6$$

where NOE_{kl} and NOE_{ij} are the NOEs between atoms *k* and *l* and atoms *i* and *j*, respectively. In the NOESY spectra of **4** and **5**, the NOE between atoms B3 and B6 of the second pyridine ring

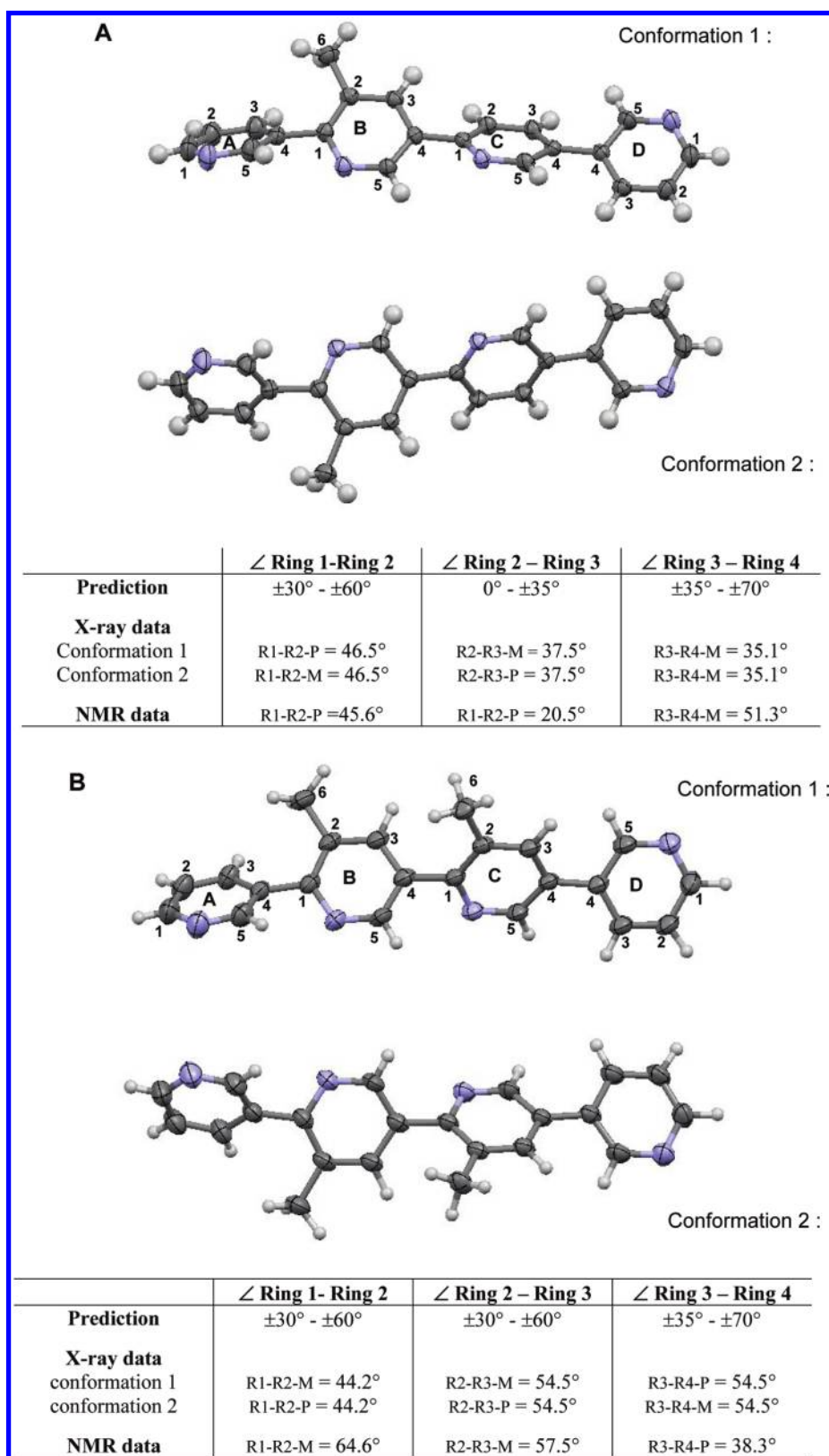


Figure 3. ORTEP view of the two conformers from crystal structures and the twist angle values of compound 4 (A) and compound 5 (B). Displacement ellipsoids are drawn at the 50% probability level, and H atoms are shown as small spheres of arbitrary radii.

(see atom numbering in Figure 3) corresponding to a distance of 0.248 nm was used for interproton distance calibration.

Thus, we have highlighted for each compound the spatial proximity of methyl group protons with protons at the α position of the adjacent cycle. Table 5 shows a comparison of the $^1\text{H}-^1\text{H}$

distances inferred from the NMR data with those obtained from the X-ray structure. Overall, pairwise comparisons show a very good match between X-ray and NMR distances.

In order to generate 3D NMR structures, we carried out molecular dynamic simulations with the NMR constraints.

Table 4. NMR Data, ^1H Chemical Shifts (ppm, CDCl_3), and ^1H – ^1H Coupling Constants (Hz)

δ ^1H (ppm)/ J (Hz)	A1	A2	A3	A5	B3	B5	B6	C2	C3	C5	C6	D1	D2	D3	D5
4	8,660 (m, 2H)	7,418 (m, 2H)	7,927 (m, 3H)	8,858 (d, 1H) $J_{\text{meta}} = 1,68$ Hz	8,333 (d, 1H) $J_{\text{meta}} = 1,56$ Hz	8,778 (d, 1H) $J_{\text{meta}} = 1,86$ Hz	2,486 (s, 3H)	7,927 (m, 3H)	8,004 (dd, 1H) $J_{\text{ortho}} = 8,19$; $J_{\text{meta}} = 2, 37$ Hz	8,955 (d, 1H) $J_{\text{meta}} = 1,86$ Hz		8,660 (m, 2H)	7,418 (m, 2H)	7,927 (m, 3H)	8,903 (d, 1H) $J_{\text{meta}} = 1,98$ Hz
5	8,655 (m, 2H)	7,419 (m, 2H)	7,938 (m, 2H)	8,860 (d, 1H) $J_{\text{meta}} = 1,80$ Hz	7,890 (d, 1H) $J_{\text{meta}} = 1,66$ Hz	8,773 (d, 2H) $J_{\text{meta}} = 1,66$ Hz	2,464 (s, 3H)		7,825 (d, 1H) $J_{\text{meta}} = 1,86$ Hz	8,783 (d, 1H) $J_{\text{meta}} = 1,86$ Hz	2,532 (s, 3H)	8,655 (m, 2H)	7,419 (m, 2H)	7,938 (m, 2H)	8,890 (d, 1H) $J_{\text{meta}} = 2,04$ Hz

Table 5. NMR Data

quaterpyridine 4			quaterpyridine 5		
NOE	distance X-ray	distance NMR	NOE	distance X-ray	distance NMR
A5/B6	4.83	3.5	A5/B6	5.03	3.4
B3/B6	3.00	3.0	C6/B5	4.84	3.0
A3/B6	2.91	3.8	C3/C6	2.97	3.0
D5/C3	2.30	3.1	A3/B6	2.75	3.7
B3/C2	4.29	2.8	B3/B6	2.93	3.0
B5/C2	4.29	2.5	B3/C6	2.98	3.5
			C5/D2	4.43	2.5
			D5/E3	2.32	2.8
			E5/D3	2.27	2.9
			C3/D2	2.07	2.7

The 10 lowest energy structures for each quaterpyridine were retained for subsequent analysis. This analysis showed that for both quaterpyridines the 10 lowest energy structures represent the same conformation. For 4 and 5, the observed NMR twist angles lie at the limits of the theoretical prediction, just as the angles from the X-ray structures do (Figure 3). This result is not surprising; we expected that the NMR structures would reproduce the twist angles' values delimited by the theoretical predictions. Moreover, the absolute values of the pyridine twist angles of the NMR and X-ray structures are very close, but the sense of rotation is not necessary the same (Figure 3). Along our theoretical calculations, the negative and positive rotations of pyridines have the same potential energy, and energy barriers of the rotations in 4 and 5 are not high (ΔE from 3 to 5.5 kcal/mol), which allows easy rotations around these pyridine junctions. The NMR helicity sense for 4, as for 5, is the same as the helicity sense of the first conformation from corresponding X-ray structures; this result seems to be a random one to us. For example, the theoretical simulation carried out on the quaterpyridines showed that for 4, when ring2 is fixed at a positive twist angle with respect to ring1 (R1–R2–P), the probability to obtain a negative (R2–R3–M) or a positive (R2–R3–P) twist of ring 3 with respect to ring 2 is almost the same; the potential energy difference of both conformations is about 0.16 kcal/mol. When R2–R3 is fixed positive, the probability to obtain a negative (R3–R4–M) or a positive (R3–R4–P) was also the same.

Our first study on oligopyridyl scaffold was carried out with small substituent, but the increase of the substituent size with the introduction of a charged atom in the substituent should influence the helicity rotation sense without necessarily introducing a chiral substituent. For example, our preliminary theoretical study with tryptophan showed that only an R1–R2–M rotation of 50° is possible in this bipyridine.

All of these results, in the solid and the liquid state, show that the predicted twist angles from the bipyridine models are reproduced in the oligopyridines. Thus, the preferential angles library computed using the bipyridine model will be a useful base to design longer chain, oligopyridines, with a desired orientation of pyridine rings, and consequently the desired orientation of the substituents on this oligopyridyl scaffold.

A superposition of conformer 1 and conformer 2 of the X-ray structure of 5 on an ideal alanine α -helix was carried out with the aim of verifying whether the positions of methyl substituents can coincide with the positions of the C β atom of the alanine side chains (see Figure 4). The oligopyridyl

scaffolds were aligned successfully along the axis of the helix. For both conformations of compound **5**, the two methyl substituents are positioned in close proximity to the side chains of i and $i + 3$ residues (see Figure 4). Thus, compound **5** will be

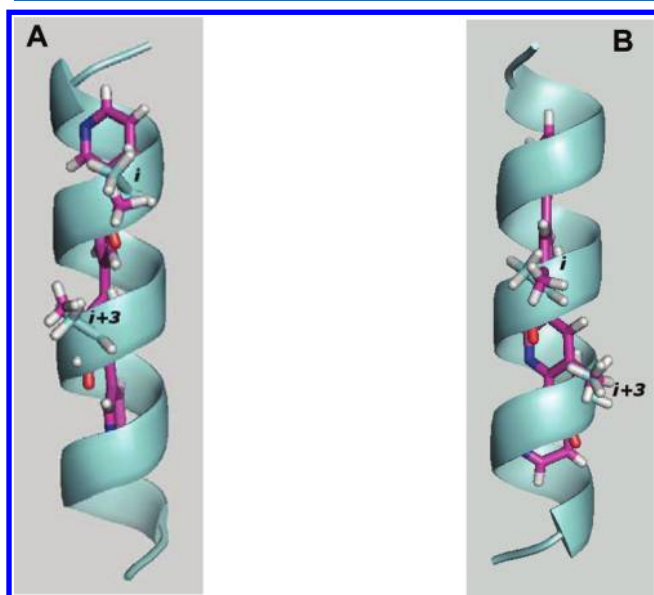


Figure 4. The superposition of the X-ray structure of conformer 1 of the compound **5** (A) and conformer 2 of the compound **5** (B) on an α helix.

able to mimic i and $i + 3$ side chains of an α helix with its substituent groups.

CONCLUSION

In our study, we assessed the ability of oligopyridyl scaffolds to mimic the α -helical twist. The first objective was to define all possible conformations associated with oligopyridines. The detailed theoretical analysis about possible conformations of bipyridines as a function of substituent and pyridine nitrogen position was carried out. Thus, the experimental structural studies confirmed the theoretical predictions, and we observed that the bipyridine conformations are maintained within a longer oligopyridyl scaffold. Furthermore, the use of an oligopyridyl scaffold gives a wider variation of consecutive ring twist (five different orientations) with respect to the oligophenyl one (two different orientations). Thus, oligopyridines allow one to play more subtly with the mutual position of the rings and so with the distribution of substituents. The present detailed study of bipyridines will be helpful in anticipating the conformational space of the designed pyridyl foldamer and orienting future syntheses. Moreover, this can be easily envisaged due to the simplicity of our synthetic methodology.

ASSOCIATED CONTENT

Supporting Information

Experimental procedures and details. This material is available free of charge via the Internet at <http://pubs.acs.org>.

AUTHOR INFORMATION

Corresponding Author

*Phone: (33)2-31-56-68-21. E-mail: jana.sopkova@unicaen.fr.

ACKNOWLEDGMENTS

We thank the CRIHAN (Centre de Ressources Informatiques de Haute Normandie) and the European Community (FEDER) for the molecular modelling software.

REFERENCES

- (1) Stockwin, L. H.; Holmes, S. Antibodies as therapeutic agents: vive la renaissance! *Expert Opin. Biol. Ther.* **2003**, *3*, 1133–1152.
- (2) Arkin, M. R.; Wells, J. A. Small-molecule inhibitors of protein-protein interactions: progressing towards the dream. *Nat. Rev. Drug Discovery* **2004**, *3*, 301–317.
- (3) Fauchère, J. L.; Thuriereau, C. Evaluation of the stability of peptides and pseudopeptides as a tool in peptide drug design. *Adv. Drug. Res.* **1992**, *23*, 128–159.
- (4) Loffet, A. Peptides as drugs: is there a market? *J. Peptide Sci.* **2002**, *8*, 1–7.
- (5) Toogood, P. L. Inhibition of protein-protein association by small molecules: approaches and progress. *J. Med. Chem.* **2002**, *45*, 1543–1558.
- (6) Clackson, T.; Wells, J. A. A Hot Spot of Binding Energy in a Hormone-Receptor Interface. *Science* **1995**, *267*, 38–386.
- (7) Jacoby, E. Biphenyls as Potential Mimetics of Protein α -Helix. *Bioorg. Med. Chem. Lett.* **2002**, *12*, 891–893.
- (8) Ruan, F. Q.; Chen, Y. Q.; Hopkins, P. B. Metal ion-enhanced helicity in synthetic peptides containing unnatural, metal-ligating residues. *J. Am. Chem. Soc.* **1990**, *112*, 9403–9404.
- (9) Horwell, D. C.; Howson, W.; Ratcliffe, G. S.; Willems, H. M. G. The Design of Dipeptide Helical Mimetics: The Synthesis, Tachykinin Receptor Affinity and Conformational Analysis of 1,1,6-Trisubstituted Indanes. *Bioorg. Med. Chem.* **1996**, *4*, 33–42.
- (10) Ahn, J.-M.; Han, S.-Y. Facile synthesis of benzamides to mimic an α -helix. *Tetrahedron Lett.* **2007**, *48*, 3543–3547.
- (11) Oguri, H.; Oomura, A.; Tanabe, S.; Hirama, M. Design and synthesis of a trans-fused polycyclic ether skeleton as an α -helix mimetic scaffold. *Tetrahedron Lett.* **2005**, *46*, 2179–2183.
- (12) Oltersdorf, T.; Elmore, S. W.; Shoemaker, A. R.; Armstrong, R. C.; Augeri, D. J.; Belli, B. A.; Bruncko, M.; Deckwerth, T. L.; Dinges, J.; Hajduk, P. J.; Joseph, M. K.; Kitada, S.; Korsmeyer, S. J.; Kunzer, A. R.; Letai, A.; Li, C.; Mitten, M. J.; Nettesheim, D. G.; Ng, S.; Nimmer, P. M.; O'Connor, J. M.; Oleksijew, A.; Petros, A. M.; Reed, J. C.; Shen, W.; Tahir, S. K.; Thompson, C. B.; Tomaselli, K. J.; Wang, B.; Wendt, M. D.; Zhang, H.; Fesik, S. W.; Rosenberg, S. H. An inhibitor of Bcl-2 family proteins induces regression of solid tumours. *Nature* **2005**, *435*, 677–681.
- (13) Yin, H.; Hamilton, A. D. Strategies for targeting protein-protein interactions with synthetic agents. *Angew. Chem., Int. Ed.* **2005**, *44*, 4130–4163.
- (14) Saraogi, I.; Hamilton, A. D. α -Helix mimetics as inhibitors of protein-protein interactions. *Biochem. Soc. Trans.* **2008**, *36*, 1414–1417.
- (15) Orner, B. P.; Ernst, J. T.; Hamilton, A. D. Toward Proteomimetics: Terphenyl Derivatives as Structural and Functional Mimics of Extended Regions of an α -Helix. *J. Am. Chem. Soc.* **2001**, *123*, 5382–5383.
- (16) Che, Y.; Brooks, B. R.; Marshall, G. R. Development of small molecules designed to modulate protein-protein interactions. *J. Comput.-Aided Mol. Des.* **2006**, *20*, 109–130.
- (17) *Discovery Studio Modeling Environment*, Release 2.0; Accelrys Software Inc.: San Diego, CA, 2005.
- (18) Frisch, M. J.; Trucks, G. W.; Schlegel, H. B.; Scuseria, G. E.; Robb, M. A.; Cheeseman, J. R.; Zakrzewski, V. G.; Montgomery, J. A., Jr.; Stratmann, R. E.; Burant, J. C.; Dapprich, S.; Millam, J. M.; Daniels, A. D.; Kudin, K. N.; Strain, M. C.; Farkas, O.; Tomasi, J.; Barone, V.; Cossi, M.; Cammi, R.; Mennucci, B.; Pomelli, C.; Adamo, C.; Clifford, S.; Ochterski, J.; Petersson, G. A.; Ayala, P. Y.; Cui, Q.; Morokuma, K.; Salvador, P.; Dannenberg, J. J.; Malick, D. K.; Rabuck, A. D.; Raghavachari, K.; Foresman, J. B.; Cioslowski, J.; Ortiz, J. V.; Baboul, A. G.; Stefanov, B. B.; Liu, G.; Liashenko, A.; Piskorz, P.; Komaromi, I.; Gomperts, R.; Martin, R. L.; Fox, D. J.; Keith, T.; Al-Laham, M. A.

Peng, C. Y.; Nanayakkara, A.; Challacombe, M.; Gill, P. M. W.; Johnson, B.; Chen, W.; Wong, M. W.; Andres, J. L.; Gonzalez, C.; Head-Gordon, M.; Replogle, E. S.; Pople, J. A. *Gaussian 98*, Revision A.11.1; Gaussian, Inc.: Pittsburgh PA, 2001.

(19) Ishikura, M.; Ohta, T.; Terashima, M. A novel synthesis of 4-aryl- and 4-heteroarylpyridines via diethyl(4-pyridyl)borane. *Chem. Pharm. Bull.* **1985**, *33*, 4755–4763.

(20) Cosford, N. D.; Kamenecka, T.; Roppe, J. R. A preparation of imidazolyl- and pyrazolyl-ethyne derivatives, useful as modulator of receptors in the nervous system. US 2005085523, 2005.

(21) Bonnet, V.; Mongin, F.; Trecourt, F.; Breton, G.; Marsais, F.; Knochel, P.; Queguiner, G. Cross-coupling between 3-pyridylmagnesium chlorides and heteroatomic halides. *Synlett* **2002**, *6*, 1008–1010.

(22) Burzicki, G.; Voisin-Chiret, A. S.; Sopkova-de Oliveira Santos, J.; Rault, S. Synthesis of dihalo bi- and terpyridines by regioselective Suzuki-Miyaura cross-coupling reactions. *Tetrahedron* **2009**, *65*, 5413–5417.

(23) Sheldrick, G. M. Phase Annealing in SHELX-90: Direct Methods for Larger Structures. *Acta Crystallogr.* **1990**, *A46*, 467–473.

(24) Sheldrick, G. M. A short history of SHELX. *Acta Crystallogr.* **2008**, *A64*, 112–122.

(25) Davis, J. M.; Truong, A.; Hamilton, A. D. Synthesis of a 2,3':6',3''-Terpyridine Scaffold as an α -Helix Mimetic. *Org. Lett.* **2005**, *7*, 5405–5408.

(26) Bouillon, A.; Lancelot, J.-C.; Collot, V.; Bovy, P.-R.; Rault, S. Synthesis of novel halopyridinylboronic acids and esters. Part 1: 6-Halopyridin-3-yl-boronic acids and esters. *Tetrahedron* **2002**, *58*, 2885–2890.

(27) Bouillon, A.; Lancelot, J.-C.; Collot, V.; Bovy, P.-R.; Rault, S. Synthesis of novel halopyridinylboronic acids and esters. Part 2: 2,4, or 5-Halopyridin-3-yl-boronic acids and esters. *Tetrahedron* **2002**, *58*, 3323–3328.

(28) Bouillon, A.; Lancelot, J.-C.; Collot, V.; Bovy, P.-R.; Rault, S. Synthesis of novel halopyridinylboronic acids and esters. Part 3: 2, or 3-Halopyridin-4-yl-boronic acids and esters. *Tetrahedron* **2002**, *58*, 4369–4373.

(29) Bouillon, A.; Lancelot, J.-C.; Sopkova-de Oliveira Santos, J.; Collot, V.; Bovy, P.-R.; Rault, S. Synthesis of novel halopyridinylboronic acids and esters. Part 4: Halopyridin-2-yl-boronic acids and esters are stable, crystalline partners for classical Suzuki cross-coupling. *Tetrahedron* **2003**, *59*, 10043–10049.

(30) Voisin, A. S.; Bouillon, A.; Berenguer, I.; Lancelot, J.-C.; Lesnard, A.; Rault, S. Novel oxybispyridylboronic acids: synthesis and study of their reactivity in Suzuki-type cross-coupling reactions. *Tetrahedron* **2006**, *62*, 11734–11739.

(31) Cailly, T.; Fabis, F.; Bouillon, A.; Lemaitre, S.; Sopkova-de Oliveira Santos, J.; Rault, S. Synthesis of orthocyanopyridylboronic acids and esters toward obtention of cyanofunctionalized bipyridines. *Synlett* **2006**, *1*, 53–56.

(32) De Giorgi, M.; Voisin-Chiret, A. S.; Sopkova-de Oliveira Santos, J.; Corbo, F.; Franchini, C.; Rault, S. Design and Synthesis of thienylpyridyl garlands as non-peptidic alpha helix mimetics and potential protein-protein interactions disruptors. *Tetrahedron* **2011**, *67*, 6145–6154.

(33) Voisin-Chiret, A. S.; Bouillon, A.; Burzicki, G.; Célant, M.; Legay, R.; El-Kashef, H.; Rault, S. A general synthesis of halo-oligopyridines. The Garlanding concept. *Tetrahedron* **2009**, *65*, 607–612.

(34) Burzicki, G.; Voisin-Chiret, A. S.; Sopkova-de Oliveira Santos, J.; Rault, S. Synthesis of New [2,3':6',3'']Terpyridines Using Iterative Cross-Coupling Reactions. *Synthesis* **2010**, *16*, 2804–2810.